



PCCP

An ARXPS and ERXPS Study of Quaternary Ammonium and Phosphonium Ionic Liquids: Utilising a High Energy Ag La' X-ray Source

Journal:	<i>Physical Chemistry Chemical Physics</i>
Manuscript ID	CP-ART-11-2015-007089.R1
Article Type:	Paper
Date Submitted by the Author:	18-Jan-2016
Complete List of Authors:	Blundell, Rebecca; University of Nottingham, School of Chemistry Delorme, Astrid; University of Nottingham, School of Chemistry Smith, Emily; The University of Nottingham, School of Chemistry Licence, Peter; The University of Nottingham, School of Chemistry

SCHOLARONE™
Manuscripts

**An ARXPS and ERXPS Study of Quaternary Ammonium and Phosphonium
Ionic Liquids: Utilising a High Energy Ag L α ' X-ray Source**

*Rebecca K. Blundell, Astrid Delorme, Emily F. Smith and Peter Licence**

*The GlaxoSmithKline Carbon Neutral Laboratory,
School of Chemistry, The University of Nottingham, Nottingham NG7 2RD, UK*

**To whom correspondence should be addressed:*

peter.licence@nottingham.ac.uk

Tel: +44 115 8466176

Introduction

Ionic liquid (IL) surface science has experienced rapid expansion in recent years. As such, a multitude of ultra-high vacuum (UHV) techniques have been used to probe the IL/vacuum interface including laboratory and synchrotron X-ray photoelectron spectroscopy (XPS),¹⁻⁷ metastable impact electron spectroscopy (MIES),⁸⁻¹⁰ low energy ion scattering (LEIS),¹¹⁻¹⁴ Rutherford backscattering (RBS)¹⁵⁻¹⁷ and neutral impact collision ion scattering spectroscopy (NICISS).¹⁸⁻²⁰ To date, the vast majority of these studies have focused upon cyclic nitrogen-containing cations, particularly the 1-alkyl-3-methylimidazolium family, whereas acyclic cations including tetraalkylammonium and –phosphonium have been overlooked despite their potential use in a wide range of existing applications including heterogeneous catalysis, gas capture/separation, and nanoparticle formation.

Clearly, the structure of the IL/vacuum interface plays a crucial role for many of these applications; therefore, it is necessary to understand how changes to the component ions can influence the IL surface, and consequently impact upon its chemistry-based applications. XPS has proved to be a robust and powerful tool for the analysis and characterisation of ionic liquid systems. Through binding energy analysis of core levels, detailed information can be extracted on the local chemical environment of an atom. XPS can also be used in the determination of chemical composition and purity of ILs and has subsequently provided many significant contributions in the areas of cation-anion interactions,²¹⁻²⁶ *in situ* reaction monitoring,^{27,28} and bulk and surface composition.^{1-7, 18, 29-31}

With the advent of commercially available high energy X-ray sources - such as Ag L α ' - energy-resolved XPS is expected to attract considerable interest over the coming years. Although ERXPS is not a new technique, it has previously required the use of synchrotron x-ray sources, which can be costly and time-limited. Consequently, the improved accessibility offered by high energy laboratory sources provides a new means to conduct ERXPS studies upon ionic liquids. This has several advantages over currently existing depth profiling techniques. Firstly, no geometry change to the sample is required, as is the case for angle-resolved XPS (ARXPS), thus enabling repeated analysis of a consistently level surface thereby minimising error caused by physical shifting of the sample. Secondly, depth profiling data can be obtained from a single experiment as opposed to repeated experiments in which the emission angle is altered (ARXPS) or photon-energy varied (synchrotron-based ERXPS); thus minimising x-ray exposure and hence sample damage. Lastly, higher energy core orbitals can be probed, elucidating further information concerning ionic liquid electronic environments, which is imperative to understanding ionic liquids at a molecular level. Accordingly, the work herein provides, to the best of our knowledge, the first description of a high energy Ag L α ' source for XPS depth profile analysis and characterisation of several ionic liquids.

Previous depth profiling studies upon ionic liquid systems have frequently used ARXPS, with few examples of ERXPS (*N.B.* limited to synchrotron sources).³¹ These investigations are again predominantly concerned with the 1-alkyl-3-methylimidazolium cation,^{1, 2, 4, 6, 30, 31} with only a handful of ARXPS studies addressing the structurally distinct pyrrolidinium cation.^{5, 31} Nevertheless, through these investigations a robust set of design rules have been established for the IL/vacuum interface of 1-alkyl-3-methylimidazolium-based ionic liquids, in which, for sufficient chain lengths ($n \geq 4$), the alkyl chains are projected towards the vacuum forming an aliphatic overlayer, with a polar sublayer of positively and negatively charged head groups residing underneath.^{1, 2, 4, 30, 31} This set of design rules also appears to hold true for the 1-alkyl-1-methylpyrrolidinium analogues;^{5, 31} however,

it would be unreasonable to simply assume that other structurally diverse cations such as the acyclic tetraalkylammonium and -phosphonium would also follow this trend. Subsequently, the work described here directly addresses this gap in knowledge to further understand the role of the cation upon the structure of the IL/vacuum interface.

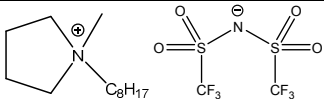
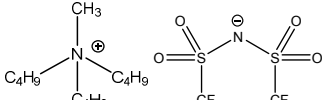
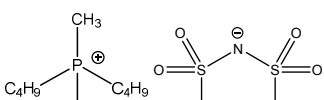
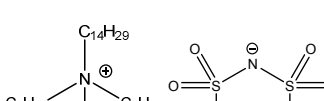
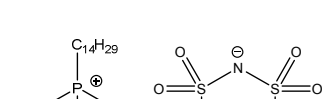
In summary, the aim of this work is to understand how the cation can influence the structure of the IL/vacuum interface through depth profiling investigations upon ionic liquids with cations of varying structural diversity including the lesser-studied tetraalkylammonium and -phosphonium cations. This is achieved by utilising the highly surface sensitive XPS techniques: ARXPS and ERXPS, to probe differences in the bulk and surface composition for the five ionic liquids studied, see Table 1. Furthermore, through a comparison of binding energies obtained *via* both the Al $K\alpha$ and Ag $L\alpha'$ x-ray sources we have provided validation for using the Ag $L\alpha'$ source to obtain robust and reliable chemical state analysis of ionic liquids, as well as characterising previously undetectable core level photoelectron emissions.

Experimental

Materials

All compounds investigated in this study were prepared in our laboratory using modified literature procedures.^{23, 32} Chemical precursors were acquired from commercial suppliers and used without further purification. Trihexyl(tetradecyl)phosphonium chloride (Cyphos IL 101) and Tributyl(methyl)phosphonium methylsulfate (Cyphos IL 108) were obtained from Cytec Industries Inc. All ionic liquids were dried *in vacuo* ($p \leq 10^{-2}$ mbar) at 50 °C and stored under argon before being fully characterised by ^1H , ^{13}C , ^{31}P and ^{19}F NMR (recorded at room temperature on a Bruker DPX-400 MHz spectrometer); IR (Perkin Elmer 1600 FT spectrometer); ESI-MS (Bruker MicroTOF 61 spectrometer) and XPS (Kratos Axis Ultra spectrometer). When anion exchange was one of the synthetic steps, ion chromatography (Dionex ICS-3000, IonPack AS15, 4 x 250 mm analytical column) showed that residual halide was below the limits of detections (< 10 ppm). Full XPS data for all ionic liquids investigated is provided within the ESI.

Table 1. Structures and abbreviations of ionic liquids investigated in this study.

Abbreviation	Structure	Name
[C ₈ C ₁ Pyrr][NTf ₂]		1-octyl-1-methylpyrrolidinium bis(trifluoromethanesulfonyl)imide
[N _{4,4,4,1}][NTf ₂]		Tributyl(methyl)ammonium bis(trifluoromethanesulfonyl)imide
[P _{4,4,4,1}][NTf ₂]		Tributyl(methyl)phosphonium bis(trifluoromethanesulfonyl)imide
[N _{6,6,6,14}][NTf ₂]		Trihexyl(tetradecyl)ammonium bis(trifluoromethanesulfonyl)imide
[P _{6,6,6,14}][NTf ₂]		Trihexyl(tetradecyl)phosphonium bis(trifluoromethanesulfonyl)imide

XPS data collection

For ARXPS studies and purity conformation a Kratos Axis Ultra spectrometer was used employing a focused, monochromated Al K α source ($h\nu = 1486.6$ eV), hybrid (magnetic/electrostatic) optics, concentric hemispherical analyser, and a multi-channel plate and delay line detector (DLD) with an X-ray incident angle of 30° (relative to the surface normal). X-ray gun power was set to 120 W. Spectra were recorded using an entrance aperture of 300 μm x 700 μm with a pass energy of 80 eV and step size 0.5 eV for survey spectra, and pass energy 20 eV and step size 0.1 eV for high resolution spectra. Survey scans were run for 1200 s and high resolutions scans for 600 s.

For ERXPS studies the Al K α source was substituted with a monochromated Ag L α' source (2984.6 eV) operated at the same power (120 W) with minor adjustments to the gun position and monochromating crystals. All spectra were recorded with an entrance aperture of 300 μm x 700 μm with pass energy of 160 eV and step size 1.0 eV for survey spectra, and pass energy of 40 eV and step size 0.2 eV for high resolution spectra. Survey scans were run for 2400 s and the high resolution scans were run for 1200 s.

Binding energy calibration was made using Au 4f_{7/2} (83.96 eV), Ag 3d_{5/2} (368.21 eV) and Cu 2p_{3/2} (932.62 eV). The resolution of the photoelectron detector was based on the Ag 3d_{5/2} peak with full width at half maximum (FWHM) of 0.55 eV at pass energy 20 eV. The Ag L α' source produces a slightly broader energy because of energy dispersion due to second order diffraction, thus Ag 3d_{5/2} FWHM is 0.9 eV. All ionic liquids investigated in this study are liquids at room temperature; therefore charge neutralisation procedures were not required as samples are conducting. Samples

were prepared by placing a small drop (≈ 10 mg) upon a stainless steel sample bar. The ionic liquids were then cast into thin films (approx. thickness 0.5 – 1.0 mm). Samples were pre-pumped in a preparative chamber to pressures lower than 1×10^{-6} mbar before transfer to the main analytical chamber. Pressure in the main chamber consistently remained $\leq 1 \times 10^{-8}$ mbar during XPS measurements, therefore all volatile impurities such as water are expected to be removed resulting in high purity samples.

XPS data analysis

Data was analysed using the CASAXPS (Version 2.3.17 dev 6.6s) software. When using the Al K α x-ray source to determine elemental composition relative sensitivity factors (RSFs) were taken from the Kratos Library (RSF F 1s = 1) and used to determine relative atomic percentages from high-resolution scans of the most intense photoelectron peak for each element. Depending on background shape a two-point linear, Shirley or linear spline background subtraction was performed to measure peak areas. Peaks were fitted using GL (30) lineshapes (70 % Gaussian, 30 % Lorentzian). For ionic liquids with a long alkyl chain ($n \geq 8$) charge-referencing was achieved by setting the experimentally determined binding energy of the aliphatic component ($C_{\text{aliphatic}}$) equal to 285.0 eV.^{22, 33} For compounds with a short alkyl chain ($n < 8$) charge-referencing was achieved by setting the measured binding energy of the cationic heteroatom photoelectron emission peak equal to that for its long chain analogue, *i.e.* $N_{\text{cation}} 1s$ for $[N_{4,4,4,1}][NTf_2]$ was set equal to 402.5 eV (where 402.5 eV is the measured binding energy for $N_{\text{cation}} 1s$ for $[N_{6,6,6,14}][NTf_2]$). A full description of charge-referencing for the ionic liquids investigated within this study can be found elsewhere in the literature.²³

ARXPS experiments at grazing emission angles ($\theta \geq 70^\circ$) give significantly lower signal intensity than experiments at normal emission angle ($\theta = 0^\circ$). Therefore, to aid visual interpretation of the ARXP spectra presented, each spectrum recorded at $\theta = 80^\circ$ is normalised to the area of the F 1s photoelectron emission peak recorded for the respective ionic liquid at $\theta = 0^\circ$. This peak was selected for normalisation as the F 1s moiety is present in all ionic liquids in the same stoichiometry, and the F 1s peak is easily identifiable with a binding energy well separated from any other photoelectron emission signals. This technique does not affect the relative ratios of different elements within the ionic liquid, thus provides a visual comparison of the same region for an ionic liquid upon changes to emission angle. Therefore, any changes in intensity of an element with emission angle can be observed.

Information depth for ARXPS and ERXPS

The information depth (ID) can be defined as the depth, within the sample, from which 95.7 % of the measured signal will originate and can be expressed as $ID = 3\lambda_{\text{AL}}\cos\theta$. For the lower energy Al K α x-ray source ID varies mainly with $\cos\theta$, where θ is the electron emission angle relative to the surface normal. At the kinetic energies measured here ($\approx 800 - 1300$ eV) the attenuation length of photoelectrons in organic compounds is of the order of $\sim 3\text{nm}$.³⁴ From this, the ID in each of the angle-resolved geometries employed in the ARXPS experiments can be estimated. Therefore, when $\theta = 0^\circ$, $ID = 7 - 9$ nm (*N.B.* this value is also dependent upon the kinetic energy of the escaping photoelectron, and therefore the identity of the element probed) and for $\theta = 80^\circ$, $ID = 1 - 1.5$ nm. It should be noted that at 80° , 65 % of the signal intensity arises from the uppermost 0.3 – 0.5 nm; this is less than the width of a single molecule for most ILs. An increase in element/component intensity

with increasing θ , and thus with increasing surface sensitivity, indicates a higher concentration of this element/component in the top most layers.

When using the higher energy Ag L α' x-ray source for ERXPS studies, a fixed normal emission angle of $\theta = 0^\circ$ is used. Consequently ID can be simplified to $ID = 3\lambda_{AL}$, thus ID is solely a function of attenuation length and hence kinetic energy. As a larger kinetic energy range is investigated $\approx 500 - 2800$ eV, ID will be very dependent upon the kinetic energy of an escaping photoelectron, and hence the core orbital from which it has originated. A full description of this technique is provided in the results and discussion section titled "Energy-Resolved XPS: Ag L α' X-ray source", however for the purpose of this section the variance in ID with different core orbitals for a specific element will be briefly described. The binding energies of S 1s and S 2p photoelectron emissions (both of which can be detected with the Ag L α' source) are respectively 2478 eV and 169 eV, corresponding to kinetic energies of 507 eV and 2816 eV. Using the NIST Effective-Attenuation-Length database the attenuation length (λ_{AL}) of S 1s and S 2p photoelectrons were estimated to be 1.4 nm and 5.3 nm respectively.³⁵ This corresponds to an S 1s ID = 4.2 nm and S 2p ID = 15.9 nm, therefore highlighting the dependence of ID upon kinetic energy for this technique. A description of this procedure including plots of λ_{AL} versus kinetic energy for each ionic liquid is provided in the ESI, it can be seen from Table S2 that λ_{AL} is not sensitive to the IL used.

Fitting procedure for C 1s region

Due to the presence of several different carbon environments peak identification and fitting of the C 1s region for ionic liquids is of particular importance. For all the ionic liquids studied herein C 1s fitting was achieved through using established models from previous studies.^{22, 23} A representative example of this procedure is described for [N_{4,4,4,1}][NTf₂], see figure 1. It can be seen that there are three peaks, two of which are unresolved. The peak at ≈ 293 eV is assigned to the $-\text{CF}_3$ group of the [NTf₂]⁻ anion. The two unresolved peaks between 284 – 288 eV arise from the different electronic environments of the cation. The peak at ≈ 285 eV is fitted with two components ($C_{\text{aliphatic}}$ and C_{inter}), and the peak at ≈ 287 eV is fitted with one component, C_{hetero} . For a full description on C 1s fitting models for pyrrolidinium and ammonium ionic liquids the reader is directed to ref. 22 and 23. The C 1s fitting model for phosphonium ionic liquids is slightly different as only two components are used to describe the distinct chemical environments of carbon in the cation, for a thorough explanation upon this family of ionic liquids the reader is also directed to ref. 23.

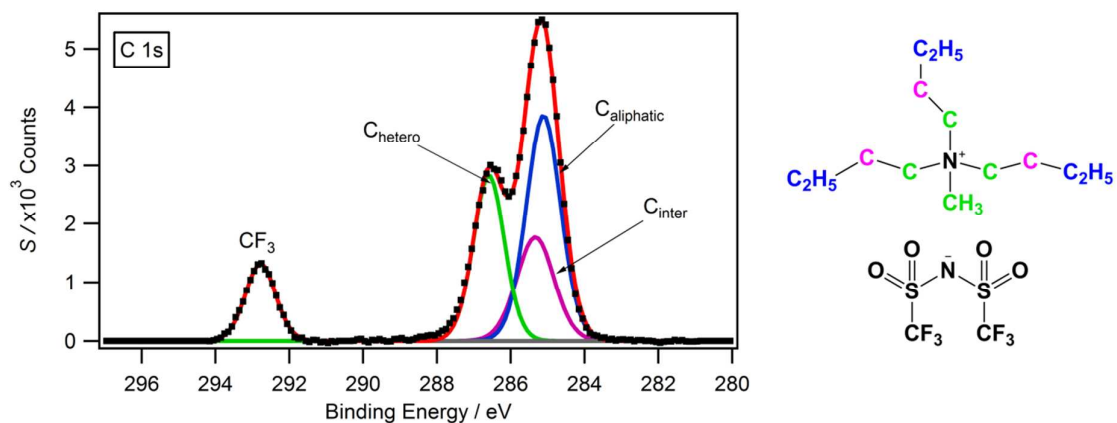


Figure 1. High resolution XP spectra of the C 1s region with component fittings for [N_{4,4,4,1}][NTf₂]. Fitting model consists of four components: CF₃, C_{hetero}, C_{inter} and C_{aliphatic}. For a full description on the development of this fitting model, see ref. 23.

Results and Discussion

Angle-Resolved XPS: Al K α X-ray source

XP spectra have been obtained at two emission angles, 0° and 80°, with respect to the surface normal for all five ionic liquids. Experimental stoichiometries were determined from the high resolution scans for each element and are presented in Table 2.

Stoichiometries determined at the electron emission angle $\theta = 0^\circ$ (ID = 7 – 9 nm) agree very well to the nominal stoichiometry and are within the experimental error for all ionic liquids studied, excluding the O 1s peak. It can be seen that the experimental O 1s stoichiometry is systematically lower than the nominal value. This suggests that the relative sensitivity factor (RSF), taken from the Kratos Library, for this element is not ideally suited for the compounds under investigation. Similar deviations in stoichiometry have been reported elsewhere.^{3, 5, 31} As this investigation is upon changes in stoichiometric ratio with respect to emission angle, small deviations in RSF values have minimal impact upon the conclusions made.

Table 2. Quantitative analysis of the XP spectra for ionic liquids studied in this work. Experimental and nominal stoichiometries (in number of atoms) are given for all constituent elements of the ionic liquids. The experimental values are obtained from XP spectra at $\theta = 0^\circ$ and 80° . Associated experimental error is $\pm 10\%$.

	Cation						Anion				
	Element	C _{aliphatic} 1s	C _{hetero} 1s	C _{inter} 1s	N _{cation} 1s	P _{cation} 2p	C _{anion} 1s	N _{anion} 1s	O 1s	S 2p	F 1s
	RSF ^{36, 37}	0.278	0.278	0.278	0.477	0.486	0.278	0.477	0.780	0.668	1.000
[C ₈ C ₁ Pyrr][NTf ₂]	Nominal	6	4	3	1	-	2	1	4	2	6
	0°	6.4	4.3	3.2	0.9	-	2.1	0.9	3.5	1.9	5.8
	80°	9.3	3.5	2.3	0.9	-	1.8	0.8	3.3	2.2	5.0
[N _{4,4,4,1}][NTf ₂]	Nominal	6	4	3	1	-	2	1	4	2	6
	0°	6.3	4.2	3.2	1.0	-	2.1	0.9	3.5	1.9	5.8
	80°	7.8	4.0	2.9	0.9	-	2.0	0.8	3.2	2.1	5.3
[P _{4,4,4,1}][NTf ₂]	Nominal	9	4	-	-	1	2	1	4	2	6
	0°	9.3	4.1	-	-	0.8	2.1	1.0	3.7	1.9	6.1
	80°	9.6	3.8	-	-	1.2	1.9	0.9	2.5	2.3	5.8
[N _{6,6,6,14}][NTf ₂]	Nominal	24	4	4	1	-	2	1	4	2	6
	0°	24.8	4.1	4.1	0.9	-	2.1	0.9	3.3	1.9	5.8
	80°	25.2	4.1	4.1	0.7	-	2.1	0.7	3.1	2.7	5.3
[P _{6,6,6,14}][NTf ₂]	Nominal	28	4	-	-	1	2	1	4	2	6
	0°	28.7	4.1	-	-	0.9	2.1	1.1	3.4	2.0	5.7
	80°	28.9	3.8	-	-	1.2	1.8	1.1	3.4	2.2	5.6

Previous ARXPS studies upon 1,3-dialkylimidazolium ionic liquids have shown a significant increase in intensity of the C_{aliphatic} 1s component with increasing emission angle, providing evidence for an enrichment of alkyl chains at the outer surface.^{1, 2, 4, 6, 7, 30, 31} A systematic investigation into this effect as a function of alkyl chain length has also shown that the degree of surface enrichment increases with the length of the alkyl chain.^{2, 4, 38}

In this study, the surface enrichment of alkyl carbon for a variety of tetraalkylammonium and phosphonium cations, including the 1-octyl-1-methylpyrrolidinium cation, is investigated using an

empirical surface enrichment factor, SE , first described by Kolbeck *et al.* in the study of imidazolium-based systems.⁶ SE is defined as the ratio of the $C_{\text{aliphatic}}$ 1s component at 80° ($ID = 1 - 1.5$ nm) to that at 0° ($ID = 7 - 9$ nm, *i.e.* representative of nominal value). Consequently, an SE value of 1.0 would indicate no surface enrichment of the alkyl chains.

For $[C_8C_1\text{Pyrr}][\text{NTf}_2]$ an SE value of 1.45 was obtained indicating a significant degree of surface enrichment of the alkyl chains, this is also illustrated by comparison of the C 1s photoelectron emission spectra obtained at 0° and 80° in Figure 2 (*N.B.* to aid visual interpretation of the presented XP spectra a normalisation procedure was applied, see experimental section for details). This behaviour is in accordance with previous ARXPS reports upon pyrrolidinium and imidazolium ionic liquids.^{2, 4, 5, 31} Furthermore, the reported SE factor for the imidazolium analogue, $[C_8C_1\text{Im}][\text{NTf}_2]$, is comparable at a value of 1.52.⁶ This suggests that the surface enrichment behaviour of pyrrolidinium- and imidazolium-based ionic liquids is very similar.

A decrease in SE is observed for $[N_{4,4,4,1}][\text{NTf}_2]$ where $SE = 1.24$ indicating that surface enrichment of alkyl carbon is less for this cation in comparison to $[C_8C_1\text{Pyrr}][\text{NTf}_2]$. This is somewhat interesting as this cation contains the same amount of alkyl carbon as $[C_8C_1\text{Pyrr}][\text{NTf}_2]$ (see Table 2) and yet does not show the same degree of carbon surface enrichment, suggesting that not all four of the alkyl chains for $[N_{4,4,4,1}][\text{NTf}_2]$ point towards the vacuum at the IL surface.

Remarkably, the SE values for the compounds $[P_{4,4,4,1}][\text{NTf}_2]$, $[N_{6,6,6,14}][\text{NTf}_2]$ and $[P_{6,6,6,14}][\text{NTf}_2]$ show almost negligible surface enrichment of alkyl carbon with SE values of 1.03, 1.02 and 1.01. This is particularly surprising for the $[N_{6,6,6,14}]^+$ and $[P_{6,6,6,14}]^+$ cations which contain a considerably large amount of aliphatic carbon. A visual comparison of the C 1s photoelectron emission at 0° and 80° for each ionic liquid studied is presented in Figure 2, highlighting the differences in surface enrichment for each cation.

A previous XPS study upon tetraalkylammonium and tetraalkylphosphonium ionic liquids investigated the influence of the cation upon anionic binding energies, in which a perceived hydrocarbon-based shielding of the cationic core for long chain cations *i.e.* $[N_{6,6,6,14}]^+$ and $[P_{6,6,6,14}]^+$ was observed.^{23, 24} We proposed this was due to the long alkyl chains wrapping around the cationic core rather than being fully extended. Furthermore, we observed that the hydrocarbon-based shielding could be reduced through a decrease in alkyl chain length or conformational restriction *i.e.* using cyclic analogues such as $[C_8C_1\text{Pyrr}][\text{NTf}_2]$.^{23, 24}

The results obtained in this study fully support this assertion as the lack of surface enrichment of alkyl carbon for $[N_{6,6,6,14}][\text{NTf}_2]$, $[P_{6,6,6,14}][\text{NTf}_2]$ and $[P_{4,4,4,1}][\text{NTf}_2]$ strongly suggests that the alkyl chains are indeed wrapped around the cation core for these cations. Also in accordance with our previous study, the effect of hydrocarbon-based shielding is clearly diminished for the cations $[C_8C_1\text{Pyrr}][\text{NTf}_2]$ and $[N_{4,4,4,1}][\text{NTf}_2]$ as evidenced by an increase in surface enrichment of alkyl carbon for these ionic liquids.

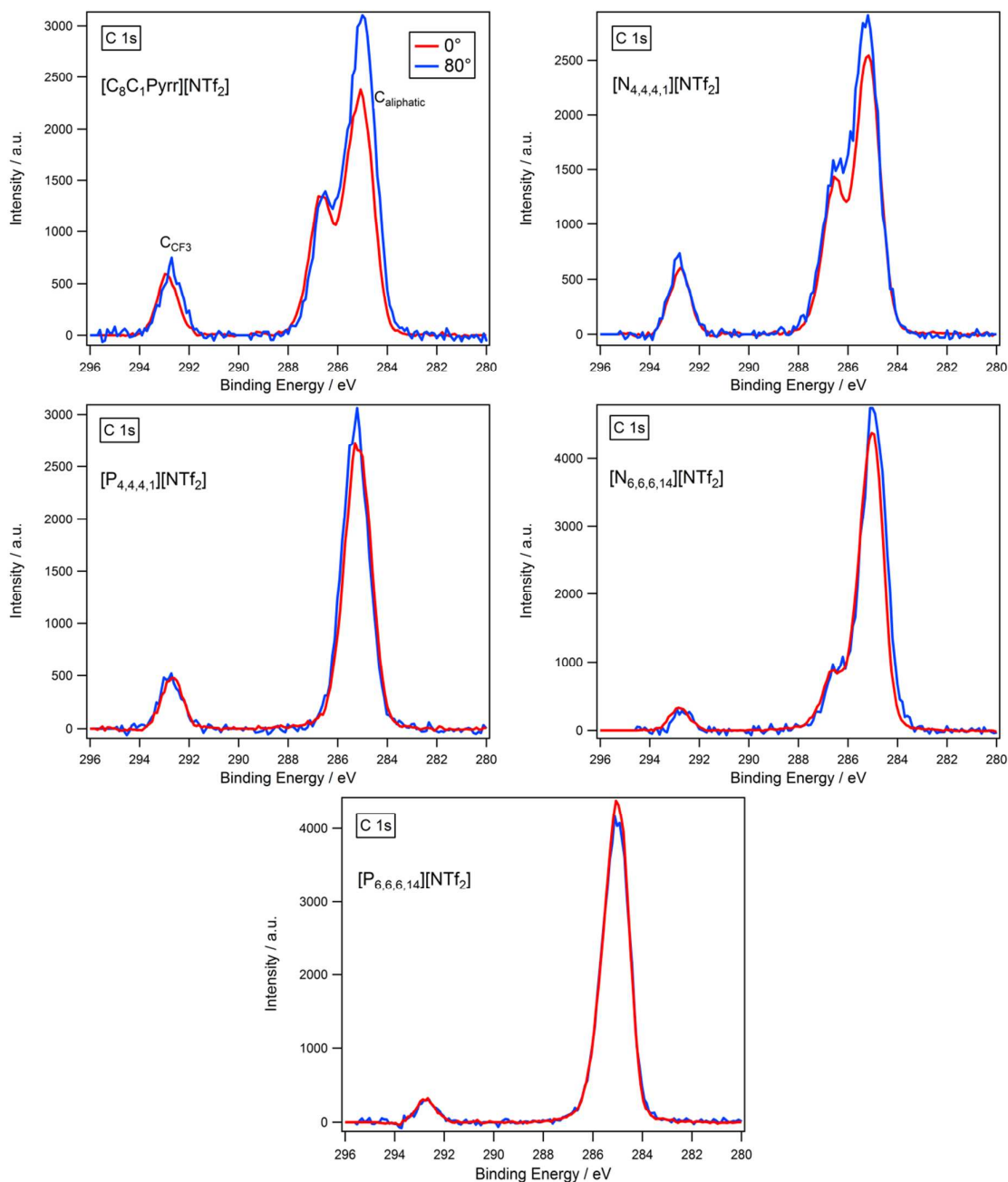


Figure 2. High resolution spectra of the C 1s region for ionic liquids studied in this work recorded at 0° (red) and 80° (blue) electron emission angle, θ , with respect to the surface normal. [C₈C₁Pyrr][NTf₂], [N_{6,6,6,14}][NTf₂] and [P_{6,6,6,14}][NTf₂] spectra charge corrected by referencing C_{aliphatic} 1s to 285.0 eV. [N_{4,4,4,1}][NTf₂] and [P_{4,4,4,1}][NTf₂] spectra were charge corrected by setting N_{cation} 1s/P_{cation} 2p_{3/2} to the value obtained for [N_{6,6,6,14}][NTf₂]/[P_{6,6,6,14}][NTf₂].

In comparison to the large surface enrichment of carbon observed for [C₈C₁Pyrr][NTf₂] where we see a 50 % increase in the C_{aliphatic} signal, more subtle effects are seen for the anionic components. Here we see a small decrease of ~15 % in the F 1s and C_{anion} 1s signals, with a corresponding ~15 % increase in the S 2p signal, Table 2. We speculate that this is the result of an orientation preference of the anion (which is situated beneath the aliphatic carbon overlayer) such that the -CF₃ groups are

pointed towards the bulk ionic liquid, away from the vacuum. A similar trend is also seen for the anionic components of the other ionic liquids studied. This supports the synchrotron-based XPS studies conducted by Lockett *et al.*³¹ on $[C_4C_1\text{Pyrr}][\text{NTf}_2]$ in which they suggest the anion, on average, has a *cis* configuration with both $-\text{CF}_3$ groups facing the bulk. A further study by Men *et al.*⁵ on a homologous series of ionic liquids of the type $[C_nC_1\text{Pyrr}][\text{NTf}_2]$ also supports this conclusion. It should be stressed that due to the liquid state of the samples, a fluid and dynamic nature exists as a result of molecular tumbling, thus the data obtained represents an average of the true situation at any time. Additionally, as this possible orientation preference of the anion exhibits a considerably smaller effect upon the ionic liquid near-surface region, in comparison to carbon surface enrichment, it is not the primary focus of this ARXPS study.

Information on the relative position of the cationic head group to the anionic head group can be obtained by measuring the change in elemental ratio for each with electron emission angle, see Table 3. It can be seen for the pyrrolidinium and ammonium ionic liquids there is very little change in ratio with emission angle indicating that cation and anion are at approximately the same distance from the interface. Interestingly for the phosphonium ionic liquids, $[P_{4,4,4,1}][\text{NTf}_2]$ and $[P_{6,6,6,14}][\text{NTf}_2]$, an increase in X / N_{anion} from 0.8 to 1.3 and 1.1 respectively is observed suggesting that the cation is located slightly above the anion.

Table 3. Elemental ratio of cationic head group X (where $X = N_{\text{cation}} 1s$ or $P_{\text{cation}} 2p$) to anionic head group ($N_{\text{anion}} 1s$) at $\theta = 0^\circ$ and 80° with an associated error of $\pm 5\%$.

Ionic Liquid	Elemental Ratios	
	$X / N_{\text{anion}} 0^\circ$	$X / N_{\text{anion}} 80^\circ$
$[C_8C_1\text{Pyrr}][\text{NTf}_2]$	1.00	1.13
$[N_{4,4,4,1}][\text{NTf}_2]$	1.11	1.13
$[P_{4,4,4,1}][\text{NTf}_2]$	0.80	1.33
$[N_{6,6,6,14}][\text{NTf}_2]$	1.00	1.00
$[P_{6,6,6,14}][\text{NTf}_2]$	0.82	1.09

In summary, $[C_8C_1\text{Pyrr}][\text{NTf}_2]$ and $[N_{4,4,4,1}][\text{NTf}_2]$ display similar behaviour at the ionic liquid/vacuum interface as previously recorded in the literature for imidazolium ionic liquids of the type $[C_nC_1\text{Im}][X]$, whereby the surface is constructed of an alkyl chain overlayer, with a sublayer of charge-bearing head groups residing underneath. However for $[N_{6,6,6,14}][\text{NTf}_2]$, $[P_{6,6,6,14}][\text{NTf}_2]$ and $[P_{4,4,4,1}][\text{NTf}_2]$ a different picture emerges, in which minimal surface ordering is present indicating a homogeneous distribution of carbon atoms in the near-surface and the bulk. This provides further evidence for the wrapping of the aliphatic chains around the cationic core for these cationic systems.

It is unclear to us at this time as to why $[P_{4,4,4,1}][\text{NTf}_2]$ also displays evidence for wrapping of alkyl chains around the cationic core, unlike its short chain ammonium analogue ($[N_{4,4,4,1}][\text{NTf}_2]$). However, a recent study by Scarbath-Evers *et al.*³⁹ has indicated a higher flexibility of bond angles and dihedral angles for phosphonium ionic liquids,³⁹ for this reason it is conceivable that the wrapping of alkyl chains around the cationic core is more likely for the short chain phosphonium cation.

Comparison of Al K α versus Ag L α' X-ray sources: Spectra and Binding Energy Analysis

To analyse the ionic liquid/vacuum interface further for the five ionic liquids studied an additional depth profiling technique has been applied which utilises a higher energy Ag L α' x-ray source ($h\nu = 2984.6$ eV). To date, XPS analysis upon ionic liquids has almost exclusively used the Al K α x-ray source ($h\nu = 1486.6$ eV); consequently, it is useful to establish a comparison between the two energy sources to affirm the capability of the Ag L α' x-ray source to provide robust chemical state analysis of ionic liquids. A comparison between the Al K α and Ag L α' x-ray source is herein described.

The main, and most important, difference between the Al K α and Ag L α' X-ray sources are their respective energies, whereby the energy of the Ag L α' X-rays are approximately twice that of the Al K α X-rays. This is well illustrated by comparison of the survey scans obtained from each source, see Figure 3. It is clear to see that the higher energy Ag L α' X-rays can not only detect the same core orbitals as the Al K α X-rays in the binding energy range 0 – 1400 eV, but also detect core orbitals at higher binding energy *i.e.* the S 1s photoelectron emission at ≈ 2500 eV.

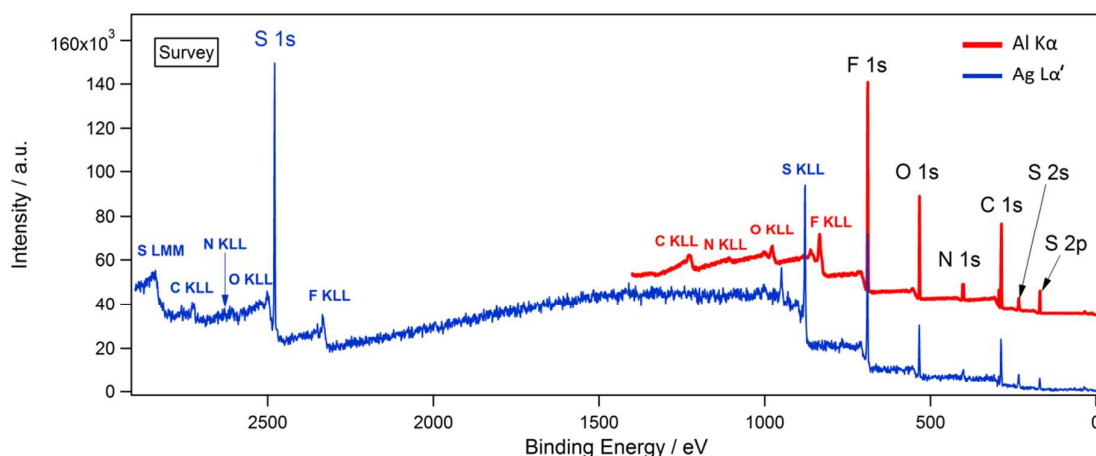


Figure 3. Survey XP spectra for $[N_{4,4,4,1}][NTf_2]$ using Al K α and Ag L α' X-ray sources. Showing photoelectron emissions detected by both sources (black labels), Auger emissions for Al source (red labels), Auger and photoelectron emissions for Ag source (blue labels). Spectra normalised to intensity of the F 1s photoemission peak obtained using the Al K α source.

The kinetic energy of an Auger emission peak is independent of the X-ray source used. Consequently, as a binding energy scale is used in an XP spectrum for the analysis of photoelectron emissions, the apparent binding energy of the Auger emissions will vary as the X-ray source is changed. This is clearly exhibited by Figure 3 where the Auger emissions using the Al K α source occur between 800 – 1400 eV, whereas the same Auger emissions occur at 2300 – 2800 eV using the Ag L α' source. As only photoelectron emissions are analysed in this study the binding energy scale is used throughout.

It should be noted that the signal intensity when using the Ag L α' source is significantly reduced in comparison to the Al K α source therefore, appropriate normalisation procedures should be used to obtain a visual comparison of spectra obtained from different sources. This arises through the Ag L α' source X-rays undergoing second order diffraction when using the same quartz crystal monochromator as the Al K α source, which undergoes first order diffraction. Subsequently, longer

acquisition times have to be employed when using the Ag L α' x-ray source to obtain spectra comparable in quality to the Al K α x-ray source, see experimental section for details.

The measured binding energies for a variety of ammonium, phosphonium and pyrrolidinium ionic liquids obtained using the Ag L α' x-ray source are presented in Table 4 and Figures S8 – S12. These values - in the range of 0 – 1400 eV - are in excellent agreement to binding energies previously obtained using the Al K α x-ray source (see table S1, supplementary information) and are within the experimental error of ± 0.1 eV. Interestingly, the measured binding energy of the F 1s photoelectron emission appears to be systematically 0.2 eV higher than that measured using the Al K α x-ray source; however, as this shift is on the upper limit of experimental error no absolute conclusion can be made. Additionally, binding energies for the higher energy P 1s and S 1s core orbitals have been characterised. Consequently, the Ag L α' x-ray source can also provide robust chemical state analysis of ionic liquids. The added value of the higher energy Ag L α' x-ray source, however, is its ability to provide a new depth profiling technique based on detecting two different core photoelectron emissions (which have a large difference in binding energy) from the same element. This will be discussed in detail in the following section.

Ionic Liquid	Binding Energy / eV											
	Cation						Anion					
	C _{aliphatic} 1s	C _{inter} 1s	C _{hetero} 1s	N _{cation} 1s	P _{cation} 1s	P _{cation} 2p _{3/2}	C _{anion} 1s	N _{anion} 1s	O 1s	F 1s	S 1s	S 2p _{3/2}
[P _{4,4,4,1}][NTf ₂]	285.1	-	285.6	-	2147.1	132.6	292.7	399.3	532.5	688.8	2478.3	168.6
[P _{6,6,6,14}][NTf ₂]	285.0	-	285.9	-	2147.2	132.6	292.8	399.4	532.6	688.9	2478.4	168.7
[N _{4,4,4,1}][NTf ₂]	285.0	285.5	286.6	402.5	-	-	292.8	399.3	532.5	688.8	2478.2	168.7
[N _{6,6,6,14}][NTf ₂]	285.0	285.8	286.8	402.5	-	-	292.9	399.4	532.6	688.9	2478.4	168.8
[C ₈ C ₁ Pyrr][NTf ₂]	285.0	285.8	286.8	402.7	-	-	292.9	399.5	532.8	689.0	2478.5	168.9

Table 4. Experimental binding energies in eV for the ionic liquids studied in this work using the Ag L α' x-ray source. The associated experimental error is \pm 0.1 eV. [N_{6,6,6,14}]⁺/ [P_{6,6,6,14}]⁺/ [C₈C₁Pyrr]⁺ compounds charge corrected by setting C_{aliphatic} 1s to 285.0 eV. [N_{4,4,4,1}]⁺/ [P_{4,4,4,1}]⁺ compounds charge corrected by setting N_{cation} 1s/P_{cation} 2p to the value obtained for the [N_{6,6,6,14}]⁺/ [P_{6,6,6,14}]⁺ analogue.

Energy-Resolved XPS: Ag L α ' X-ray source

As previously mentioned a depth profile of an element within an ionic liquid can be obtained if two core photoelectron emissions from that element can be detected, most importantly they must also have a wide separation in energy. By using the higher energy Ag L α ' x-ray source photoelectron emissions at higher binding energy can be detected, Figure 3. From this it can be seen that a depth profile can be obtained for the sulfur atom of the [NTf₂]⁻ anion for each ionic liquid through comparison of the S 1s and S 2p photoelectron peaks. It is important to note that this approach does not require any geometry change to the sample, *i.e.* all spectra are recorded at a fixed emission angle where $\theta = 0^\circ$, consequently any error introduced by a change in geometry is removed.

This technique, termed Energy-Resolved XPS (ERXPS), is based on the fact that the depth from which a photoelectron is able to escape is dependent upon the kinetic energy of the photoelectron. A higher kinetic energy will allow the photoelectron to travel for a longer distance in the sample without experiencing energy loss through collisions *i.e.* it has a longer attenuation length, λ_{AL} .

From Table 4 the binding energies for S 2p and S 1s core orbitals for all ionic liquids studied are respectively ≈ 169 eV and 2478 eV. This corresponds to kinetic energies of S 2p ≈ 2816 eV and S 1s ≈ 507 eV. Consequently, a photoelectron emitted from the S 2p orbital has a greater probability of escaping from deeper in the sample than an S 1s photoelectron. The NIST Electron Effective-Attenuation-Length database was used to estimate λ_{AL} using the TPP-2M method for S 2p and S 1s photoelectrons for each ionic liquid studied to give approximate values of 5.3 nm and 1.4 nm respectively, see ESI for a full description of this procedure alongside estimated λ_{AL} values for each ionic liquid.³⁵

The information depth (ID = 3 λ_{AL}) is defined as the depth, within the sample, from which 95.7 % of the measured signal will originate. It should be noted that attenuation length is used to describe the depth rather than inelastic mean free path (λ_{IMFP}) as it does not include elastic scattering events which can cause overestimated depth. Attenuation length is typically 20 % smaller than IMFP, and has been accounted for in the work described herein.^{40, 41}

Information depths were obtained using the calculated λ_{AL} values to give an S 1s ID = 4.2 nm and S 2p ID = 15.9 nm. Consequently, the S 2p signal gives a "bulk sensitive" representation of the sulfur concentration in the sample, in contrast to the S 1s signal which gives a "surface sensitive" representation. Due to the different cross-sections of the two sulfur orbitals (S 2p and S 1s), and hence different RSF values, a direct comparison of peak areas does not provide quantitative information upon sulfur surface enrichment within a sample. To achieve this, the area ratio of S 2p : S 1s must first be determined for a homogeneously disordered ionic liquid sample, this can then be used to construct the currently unknown RSF for the S 1s peak by multiplication of the known S 2p RSF by the appropriate factor (obtained from area ratio of S 2p : S 1s). Once attained the S 1s and S 2p signals can be quantified and directly compared for any sample, thus providing a measure of sulfur surface enrichment. However, as previously discussed many ionic liquids show significant surface ordering and therefore do not contain a homogeneous distribution of ions, thus the confirmation of an appropriate ionic liquid standard is currently underway in our laboratories.

As such, in this work a qualitative approach is used to determine differences in sulfur surface enrichment between samples. By comparison of the peak area ratio of S 2p : S 1s between different

samples a relative depth profile can be obtained, whereby the area for S 2p is effectively constant (as it is representative of the bulk) and the area for S 1s will vary with surface enrichment of sulfur thus affecting the ratio of S 2p : S 1s accordingly for each sample. Therefore, a comparison of this ratio between different samples will show any differences in sulfur surface enrichment relative to each other. In parallel with the ARXPS study, $[\text{C}_8\text{C}_1\text{Pyrr}][\text{NTf}_2]$ was investigated by ERXPS as a reference as the surface enrichment and orientation preferences for this compound are well defined in the literature by many different techniques.^{5, 13, 31, 42-44} Subsequently, it has been seen from these investigations that the surface structure for pyrrolidinium ionic liquids is analogous to their related imidazolium compounds; thus it is expected that the trends exhibited by the pyrrolidinium cation in ERXPS would also prove representative for the imidazolium analogue.

The S 2p and S 1s peak areas for each ionic liquid studied were measured from the respective survey spectra with an average taken for three different positions on the sample to obtain the peak area ratio as presented in Table 5.

Table 5. Ratio of S 2p to S 1s photoelectron emission peak area for the ionic liquids studied in this work. Areas measured from survey spectra with an associated error of $\pm 5\%$.

Ionic Liquid	Photoelectron emission peak area
	S 2p : S 1s
$[\text{N}_{4,4,4,1}][\text{NTf}_2]$	1 : 20.5
$[\text{C}_8\text{C}_1\text{Pyrr}][\text{NTf}_2]$	1 : 17.7
$[\text{P}_{4,4,4,1}][\text{NTf}_2]$	1 : 14.1
$[\text{N}_{6,6,6,14}][\text{NTf}_2]$	1 : 13.9
$[\text{P}_{6,6,6,14}][\text{NTf}_2]$	1 : 13.8

It is apparent that the concentration of the $[\text{NTf}_2]^-$ anion in the near-surface region appears highly dependent upon the structure of the cation. A greater surface presence of sulfur is observed for $[\text{N}_{4,4,4,1}][\text{NTf}_2]$ as the ratio of S 1s to S 2p is largest, this is closely followed by $[\text{C}_8\text{C}_1\text{Pyrr}][\text{NTf}_2]$. In contrast, the ionic liquids $[\text{N}_{6,6,6,14}][\text{NTf}_2]$, $[\text{P}_{6,6,6,14}][\text{NTf}_2]$ and $[\text{P}_{4,4,4,1}][\text{NTf}_2]$ all have a similar S 2p : S 1s ratio which is significantly lower than the values obtained for $[\text{N}_{4,4,4,1}][\text{NTf}_2]$ and $[\text{C}_8\text{C}_1\text{Pyrr}][\text{NTf}_2]$, thus corresponding to a decrease in surface concentration of the sulfur atom of the $[\text{NTf}_2]^-$ anion. It is interesting how this difference in behaviour mirrors the trend observed in the angle-resolved studies upon these ionic liquids as discussed previously.

An explanation for the differences in surface concentration of the $[\text{NTf}_2]^-$ sulfur in the near-surface region can be provided through considering the difference in ordering at the ionic liquid/vacuum interface for these ionic liquids. As discussed in the section "Angle-Resolved XPS: Al K α X-ray source" for $[\text{N}_{4,4,4,1}][\text{NTf}_2]$ and $[\text{C}_8\text{C}_1\text{Pyrr}][\text{NTf}_2]$ the surface is constructed of an alkyl chain overlayer, with a sublayer of charge-bearing head groups residing underneath. Therefore, the sulfur enrichment for $[\text{N}_{4,4,4,1}][\text{NTf}_2]$ and $[\text{C}_8\text{C}_1\text{Pyrr}][\text{NTf}_2]$ may arise through detection of the ionophilic sublayer of charged head groups which reside underneath the alkyl overlayer.

However, in the case of $[\text{N}_{6,6,6,14}][\text{NTf}_2]$, $[\text{P}_{6,6,6,14}][\text{NTf}_2]$ and $[\text{P}_{4,4,4,1}][\text{NTf}_2]$ angle-resolved studies indicate that no such ordering occurs at the ionic liquid/vacuum interface and a homogeneous distribution of ions exists. This is supported by a reduction of the S 2p : S 1s ratio, which indicates a

reduction in surface concentration of sulfur, and hence a greater proportion of the sulfur signal arises from the bulk. Furthermore, as both ARXPS and ERXPS studies upon these ionic liquids provide evidence for a homogeneous distribution of ions, they could be used in future as an appropriate reference sample to estimate the S 1s RSF. This would enable quantitative data on sulfur surface enrichment to be obtained through future ERXPS investigations. RSFs for these samples are not reported here as this study is limited to only a small subset of ILs. The perceived value of RSFs derived from such a small sample size is not great, however we are currently collecting data to make a comprehensive comparison of RSFs possible.

Overall, the data obtained through ERXPS is not only supportive to ARXPS studies, but also additive to it. It is apparent that the surface ordering of the $[\text{NTf}_2]^-$ anion is very dependent upon cation structure, in which sulfur surface enrichment occurs for $[\text{C}_8\text{C}_1\text{Pyrr}][\text{NTf}_2]$ and $[\text{N}_{4,4,4,1}][\text{NTf}_2]$, and in corroboration with an ARXPS investigation it provides further evidence for the wrapping of alkyl chains around the cationic core for long chain ammonium and phosphonium systems.

Conclusion

Two depth profiling techniques (ARXPS and ERXPS) have been used to probe the cationic influence on the structure of the ionic liquid/vacuum interface. An ARXPS study has shown that the degree of alkyl surface enrichment is dependent upon the type of cation used, whereby it is largest for constrained or short chain ammonium cations. However, in the case of long chain ammonium and phosphonium systems, and also a short chain phosphonium analogue, minimal surface ordering is observed, providing further evidence for the wrapping of alkyl chains around the cationic core in these systems, resulting in a homogeneous distribution of ions.

Additionally, we have described the use of an Ag $\text{L}\alpha'$ x-ray source for ionic liquid analysis. A comparison of binding energies obtained *via* this source against the Al $\text{K}\alpha$ source has been made and indicate that the Ag $\text{L}\alpha'$ source also provides robust chemical state analysis for ionic liquids, alongside characterising higher energy core photoelectron emissions *i.e.* S 1s and P 1s.

Furthermore, we have demonstrated the use of the Ag $\text{L}\alpha'$ x-ray source in providing another depth profiling technique, ERXPS, to measure the depth profile of the sulfur atom of the $[\text{NTf}_2]^-$ anion. A cationic dependence upon surface ordering of the anion was demonstrated, with similar trends observed as to those obtained through ARXPS. It was found that both depth profiling techniques were supportive and additive to each other and provide evidence for a hydrocarbon-based shielding of the cationic core for cations of the type $[\text{N}_{6,6,6,14}]^+$, $[\text{P}_{6,6,6,14}]^+$, and $[\text{P}_{4,4,4,1}]^+$, in contrast to $[\text{C}_8\text{C}_1\text{Pyrr}]^+$ and $[\text{N}_{4,4,4,1}]^+$ where the alkyl chains are extended away from the cationic core.

Acknowledgements

We thank the EPSRC (EP/K005138/1) for financial support and for provision of the Ionic Liquids XPS Facility. We gratefully acknowledge the Nottingham Nanotechnology and Nanoscience Centre (NNNC) XPS service. We also thank Cytec Inc. for the kind donation of samples of Cyphos 101 and Cyphos 108 precursor materials. RKB acknowledges the University of Nottingham for financial support.

References

1. C. Kolbeck, T. Cremer, K. R. J. Lovelock, N. Paape, P. S. Schulz, P. Wasserscheid, F. Maier and H.-P. Steinrück, *J. Phys. Chem. B*, 2009, **113**, 8682-8688.
2. K. R. J. Lovelock, C. Kolbeck, T. Cremer, N. Paape, P. S. Schulz, P. Wasserscheid, F. Maier and H.-P. Steinrück, *J. Phys. Chem. B*, 2009, **113**, 2854-2864.
3. C. Kolbeck, M. Killian, F. Maier, N. Paape, P. Wasserscheid and H.-P. Steinrück, *Langmuir*, 2008, **24**, 9500-9507.
4. F. Maier, T. Cremer, C. Kolbeck, K. R. J. Lovelock, N. Paape, P. S. Schulz, P. Wasserscheid and H.-P. Steinrück, *Phys. Chem. Chem. Phys.*, 2010, **12**, 1905-1915.
5. S. Men, B. B. Hurisso, K. R. J. Lovelock and P. Licence, *Phys. Chem. Chem. Phys.*, 2012, **14**, 5229-5238.
6. C. Kolbeck, A. Deyko, T. Matsuda, F. T. U. Kohler, P. Wasserscheid, F. Maier and H. P. Steinrück, *Chemphyschem*, 2013, **14**, 3726-3730.
7. C. Kolbeck, I. Niedermaier, A. Deyko, K. R. J. Lovelock, N. Taccardi, W. Wei, P. Wasserscheid, F. Maier and H.-P. Steinrück, *Chem. Eur. J.*, 2014, **20**, 3954-3965.
8. T. Iwahashi, T. Nishi, H. Yamane, T. Miyamae, K. Kanai, K. Seki, D. Kim and Y. Ouchi, *J. Phys. Chem. C*, 2009, **113**, 19237-19243.
9. S. Krischok, M. Eremtchenko, M. Himmerlich, P. Lorenz, J. Uhlig, A. Neumann, R. Ottking, W. J. D. Beenken, O. Hofft, S. Bahr, V. Kempter and J. A. Schaefer, *J. Phys. Chem. B*, 2007, **111**, 4801-4806.
10. O. Hofft, S. Bahr, M. Himmerlich, S. Krischok, J. A. Schaefer and V. Kempter, *Langmuir*, 2006, **22**, 7120-7123.
11. S. Caporali, U. Bardi and A. Lavacchi, *J. Electron Spectrosc. Relat. Phenom.*, 2006, **151**, 4-8.
12. A. Kauling, G. Ebeling, J. Morais, A. Padua, T. Grehl, H. H. Brongersma and J. Dupont, *Langmuir*, 2013, **29**, 14301-14306.
13. I. J. Villar-Garcia, S. Fearn, G. F. De Gregorio, N. L. Ismail, F. J. V. Gschwend, A. J. S. McIntosh and K. R. J. Lovelock, *Chem. Sci.*, 2014, **5**, 4404-4418.
14. I. J. Villar-Garcia, S. Fearn, N. L. Ismail, A. J. S. McIntosh and K. R. J. Lovelock, *Chem. Commun.*, 2015, **51**, 5367-5370.
15. K. Nakajima, A. Ohno, M. Suzuki and K. Kimura, *Nucl. Instrum. Methods Phys. Res. Sect. B.*, 2009, **267**, 605-609.
16. K. Nakajima, A. Ohno, H. Hashimoto, M. Suzuki and K. Kimura, *J. Chem. Phys.*, 2010, **133**, 7.
17. K. Nakajima, M. Miyashita, M. Suzuki and K. Kimura, *J. Chem. Phys.*, 2013, **139**, 8.
18. T. Hammer, M. Reichelt and H. Morgner, *Phys. Chem. Chem. Phys.*, 2010, **12**, 11070-11080.
19. C. Ridings, V. Lockett and G. Andersson, *Phys. Chem. Chem. Phys.*, 2011, **13**, 17177-17184.
20. C. Ridings, G. G. Warr and G. G. Andersson, *Phys. Chem. Chem. Phys.*, 2012, **14**, 16088-16095.
21. T. Cremer, C. Kolbeck, K. R. J. Lovelock, N. Paape, R. Wolfel, P. S. Schulz, P. Wasserscheid, H. Weber, J. Thar, B. Kirchner, F. Maier and H.-P. Steinrück, *Chem. Eur. J.*, 2010, **16**, 9018-9033.
22. S. Men, K. R. J. Lovelock and P. Licence, *Phys. Chem. Chem. Phys.*, 2011, **13**, 15244-15255.
23. R. K. Blundell and P. Licence, *Phys. Chem. Chem. Phys.*, 2014, **16**, 15278 - 15288.
24. R. K. Blundell and P. Licence, *Chem. Commun.*, 2014, **50**, 12080-12083.
25. A. R. Santos, R. K. Blundell and P. Licence, *Phys. Chem. Chem. Phys.*, 2015, **17**, 11839-11847.
26. I. J. Villar-Garcia, K. R. J. Lovelock, S. Men and P. Licence, *Chem. Sci.*, 2014, **5**, 2573-2579.
27. I. Niedermaier, C. Kolbeck, N. Taccardi, P. S. Schulz, J. Li, T. Drewello, P. Wasserscheid, H.-P. Steinrück and F. Maier, *ChemPhysChem*, 2012, **13**, 1725-1735.
28. C. Kolbeck, I. Niedermaier, N. Taccardi, P. S. Schulz, F. Maier, P. Wasserscheid and H.-P. Steinrück, *Angew. Chem. Int. Edition.*, 2012, **51**, 2610-2613.
29. F. Maier, J. M. Gottfried, J. Rossa, D. Gerhard, P. S. Schulz, W. Schwieger, P. Wasserscheid and H. P. Steinrück, *Angewandte Chemie-International Edition*, 2006, **45**, 7778-7780.
30. V. Lockett, R. Sedev, C. Bassell and J. Ralston, *Phys. Chem. Chem. Phys.*, 2008, **10**, 1330-1335.

31. V. Lockett, R. Sedev, S. Harmer, J. Ralston, M. Horne and T. Rodopoulos, *Phys. Chem. Chem. Phys.*, 2010, **12**, 13816-13827.
32. A. Cieniecka-Roslonkiewicz, J. Pernak, J. Kubis-Feder, A. Ramani, A. J. Robertson and K. R. Seddon, *Green Chem.*, 2005, **7**, 855-862.
33. I. J. Villar-Garcia, E. F. Smith, A. W. Taylor, F. L. Qiu, K. R. J. Lovelock, R. G. Jones and P. Licence, *Phys. Chem. Chem. Phys.*, 2011, **13**, 2797-2808.
34. R. F. Roberts, D. L. Allara, C. A. Pryde, N. E. Buchanan and N. D. Hobbins, *Surf. Interface. Anal.*, 1980, **2**, 5-10.
35. C. J. Powell and A. Jablonski, *NIST Electron Effective-Absorption-Length Database - Version 1.3*, National Institute of Standards and Technology, Gaithersburg, MD, 2011.
36. E. F. Smith, F. J. M. Rutten, I. J. Villar-Garcia, D. Briggs and P. Licence, *Langmuir*, 2006, **22**, 9386-9392.
37. C. D. Wagner, L. E. Davis, M. V. Zeller, J. A. Taylor, R. H. Raymond and L. H. Gale, *Surf. Interface Anal.*, 1981, **3**, 211-225.
38. H. P. Steinruck, *Phys. Chem. Chem. Phys.*, 2012, **14**, 5010-5029.
39. L. K. Scarbath-Evers, P. A. Hunt, B. Kirchner, D. R. MacFarlane and S. Zahn, *Phys. Chem. Chem. Phys.*, 2015, **17**, 20205-20216.
40. J. F. Watts and J. Wolstenholme, *An Introduction to Surface Analysis by XPS and AES*, John Wiley & Sons Ltd, Great Britain, first edition edn., 2003.
41. D. Briggs and J. T. Grant, *Surface Analysis by Auger and X-ray Photoelectron Spectroscopy*, IM Publications LLP, Manchester, 2003.
42. X. Paredes, J. Fernandez, A. A. H. Padua, P. Malfreyt, F. Malberg, B. Kirchner and A. S. Pensado, *J. Phys. Chem. B*, 2014, **118**, 731-742.
43. C. Aliaga, G. A. Baker and S. Baldelli, *J. Phys. Chem. B*, 2008, **112**, 1676-1684.
44. A. M. Smith, K. R. J. Lovelock and S. Perkin, *Faraday Discuss.*, 2013, **167**, 279-292.